Cooling of a Zero-Nuclear-Spin Molecular Ion to a Selected Rotational State

Patrick R. Stollenwerk,[1,*] Ivan O. Antonov,[2,*] Sruthi Venkataramanababu,[3] Yen-Wei Lin,[2] and Brian C. Odom[2,†]
[1]Argonne National Laboratory, Lemont, Illinois 60439, USA
[2]Department of Physics and Astronomy, Northwestern University, Evanston, Illinois 60208, USA
[3]Graduate Program in Applied Physics, Northwestern University, Evanston, Illinois 60208, USA

(Received 19 May 2020; accepted 10 August 2020; published 9 September 2020)

We demonstrate rotational cooling of the silicon monoxide cation via optical pumping by a spectrally filtered broadband laser. Compared with diatomic hydrides, SiO^+ is more challenging to cool because of its smaller rotational interval. However, the rotational level spacing and the large dipole moment of SiO^+ allows for direct manipulation by microwaves, and the absence of hyperfine structure in its dominant isotopologue greatly reduces demands for pure quantum state preparation. These features make $^{28}Si^{16}O^+$ a good candidate for future applications such as quantum information processing. Cooling to the ground rotational state is achieved on a 100 ms timescale and attains a population of 94(3)%, with an equivalent temperature $T = 0.53(6)$ K. We also describe a novel spectral-filtering approach to cool into arbitrary rotational states and use it to demonstrate a narrow rotational population distribution ($N \pm 1$) around a selected state.

DOI: 10.1103/PhysRevLett.125.113201

Introduction.—A broad range of physics and chemistry interest motivates developing tools for robust control over molecular internal degrees of freedom. Applications include study of cold collisions [1,2], quantum state-dependent chemistry [3–5], astrochemistry [6], many-body physics [7–10], quantum information processing [11–13], and precision spectroscopy [14–18]. Molecules, in contrast to free atoms, have rotational and vibrational degrees of freedom via their chemical bonds. On one hand, these extra degrees of freedom extend the scope of possible control and provide the rich structure that generates their appeal. On the other hand, their level structure can be quite complicated and thus challenging for state control. Despite this increased complexity, substantial progress on state preparation of molecules has been made in the past decade using several techniques including optical pumping [19–23], buffer-gas cooling [24,25], state-selective photoionization [26], projective preparation using quantum logic [27], supersonic expansion of molecular beams [28], and photoassociation [29].

Trapped molecular ions in Coulomb crystals can be isolated from the environment and are well suited for precision spectroscopy, quantum information processing, and other applications requiring uninterrupted dynamics over long timescales. State preparation by optical pumping allows for rapid resetting of the molecular state, often desired in these applications. Optical pumping of trapped molecular ion rotations has previously been demonstrated for diatomic hydrides [20,21,23]. However, the nonzero nuclear spin of hydrogen (or deuterium) couples with the rotational degree of freedom and any nuclear spin of the other atom, making optical pumping to a pure state still a challenge. The only demonstration of simultaneous rotational and nuclear spin optical pumping achieved ∼20% hyperfine state purity of HD^+ in a few tens of seconds [30]. A somewhat different quantum-logic approach heralds with high confidence the pure state into which it projects a trapped CaH^+ ion, but the *a priori* probability of being in a given rotational manifold is currently limited to the ∼10% thermal population [27].

In contrast to hydrides, high natural-abundance oxide isotopologues exist where both atoms have nuclear spin $I = 0$, circumventing the challenge of hyperfine structure in quantum state preparation. Taking advantage of this simplification, we demonstrate here broadband optical pumping of $^{28}Si^{16}O^+$ to its ground rotational level, with well-defined total angular momentum, on a timescale of 100 ms with 94(3)% fidelity. We also demonstrate, although with lower state purity, optical pumping to a selected rotational state with $N > 0$.

The rotational spacing of oxides (43 GHz for the lowest SiO^+ interval) is smaller than the few to several hundred GHz typical of hydrides. This makes cooling oxides more challenging, both because the optical pumping spectrum is more congested and because more levels are thermally populated; 95% of the 300 K population is distributed over the rotational states $N \leq 30$ for SiO^+, compared with ∼10 for typical hydrides. Although technically more challenging for cooling, the smaller rotational interval of oxides is favorable for future applications. SiO^+ has a sizeable body-frame dipole moment of > 4 Debye [31–34], so coherent rotational transitions can be driven with convenient microwave sources. Also rotational transitions of oxides are further from the peak of the 300 K blackbody spectrum, so

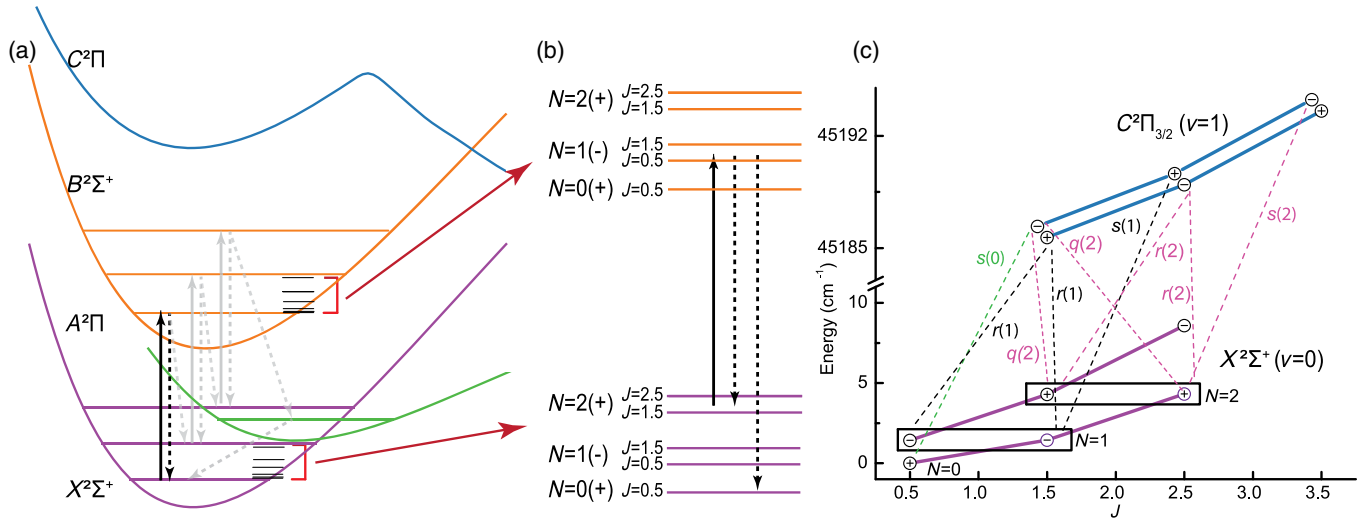

FIG. 1. Transitions for pumping and state readout. (a) Potential energy curves (not to scale) for the lowest three electronic states along with the higher-lying C state, with representative vibrational and rotational substructure. Black arrows show the primary pumping excitation and spontaneous emission channel, and gray arrows a possible parity flip sequence. (b) Rotational pumping from $N = 2 \rightarrow 0$. (c) Dissociative transitions from $N = 0, 1, 2$.

ultimate lifetimes and coherence times for polar oxides can be one to three orders of magnitude longer, depending on other limiting factors.

Broadband optical pumping.—At 300 K, 99.6% of SiO^+ molecules are in the ground vibrational state $v = 0$, but population is spread over ~30 rotational levels. We desire rotational pumping that minimizes unwanted incidental vibrational excitations. Several groups have noted the advantage of optical pumping with the class of molecules whose ground and excited electronic states have similar bond equilibrium distances, i.e., molecules with nearly diagonal Franck-Condon factors (FCFs) [22,35–38]. Such molecules have electronic excitation largely decoupled from vibrational excitation. In SiO^+ the diagonal FCFs of the B-X transition [Fig. 1(a)] allow on average more than 30 optical pumping cycles before v changes [39].

Diagonal FCFs also imply that the states have nearly identical rotational constants, resulting in a spectrum well separated according to angular momentum selection rules. A broadband laser with relatively simple spectral filtering tuned to a diagonal transition in AlH^+ was used to achieve high-fidelity cooling to the ground rotational state [23]. Since the rotational constant of SiO^+ is an order of magnitude smaller, rotational cooling of this new species to a similar degree requires significantly better spectral filtering.

State preparation of SiO^+ was achieved by spectrally filtering a frequency doubled Spectra-Physics MaiTai HP laser tuned to the $B^2\Sigma^+ - X^2\Sigma^+$ electronic transition near 385 nm. Spectral filtering was done by using the 2-f configuration of the pulse-shaping setup described in [40]. For ground state preparation the spectral filtering mask requires pumping of only the P-branch transitions ($\Delta N = -1$), which is accomplished by blocking the high frequency components at the Fourier plane with a razor blade (Fig. 2) [23,41].

To extend preparation to arbitrary $N > 0$ rotational states, a mask on the P branch must be introduced to only pump down to the target state, and the mask on the R branch needs to be shifted to allow pumping up to the target state (Fig. 2). This is accomplished with the removal of a band in the middle of the spectrum in addition to the removal of the high frequency components. This band is filtered using a thin metal ribbon (0.038×3 mm) whose profile is adjusted by rotating to match the required bandwidth at the Fourier plane. In this way, each rotational level is exclusively pumped toward the target state, which is intentionally left dark.

Trapping and detection.—Quantum state control experiments were performed at room temperature under ultrahigh vacuum conditions [$7(4) \times 10^{-10}$ Torr]. For each data point a sample of 10 to 100 SiO^+ was coloaded with 500 to 1000 laser cooled barium ions in a linear Paul trap. Loading of SiO^+ was performed using the SiO $A^1\Pi - X^1\Sigma^+(5, 0)$ 1 + 1 REMPI transition following ablation of a solid SiO sample [42]. Translational energy is rapidly cooled sympathetically by Ba^+, however molecular internal degrees of freedom are decoupled from translational motion. We expect to load SiO^+ between $N = 4$ and $N = 15$ [42]. The interval between loading and dissociation is typically 30 s at which time, without optical pumping, BBR and spontaneous emission have redistributed the population from a single N into nearby levels, but full thermal equilibration has not yet occurred. We do not observe significant population in $N = 0$ without optical pumping.

The trapped SiO^+ were detected using an *in situ* laser cooled fluorescence mass spectrometry (LCFMS) [43]

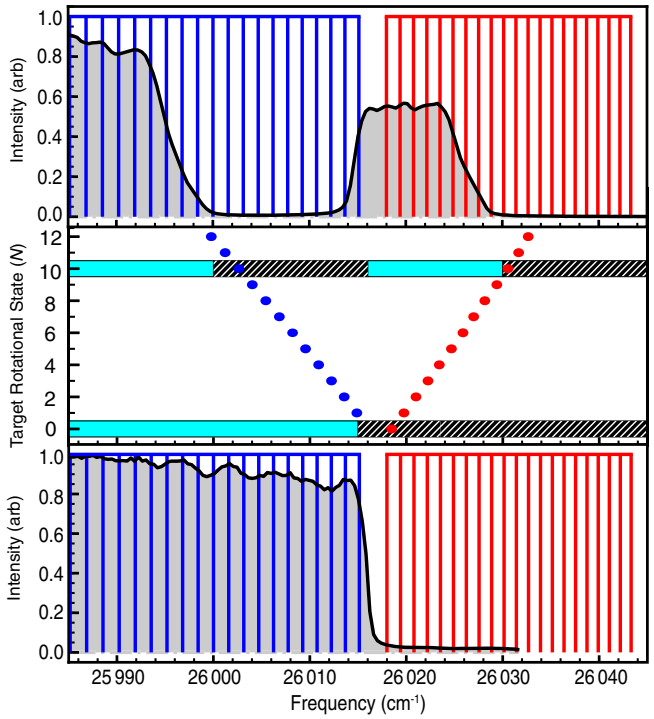

FIG. 2. Center: spectral masks overlayed onto the Fortrat diagram of the SiO^+ $B-X(0,0)$ transition. P- and R-branch transitions are indicated by blue and red dots, respectively. The blocked spectrum for each mask is indicated by the dark hashes. The measured optical pumping spectra which have been filtered to target the ground rotational state (bottom) and $N=10$ (top) are shown with the relevant P- and R-branch transitions indicated by blue and red vertical lines.

technique. Briefly, the radial secular motion of the SiO^+ was resonantly excited using a low amplitude (0.5–1 V) RF waveform applied to one of the radial trapping rods. Motional excitation causes Doppler broadening of the Ba^+ resonance and a decrease of Ba^+ fluorescence in proportion to the number of SiO^+ in the trap.

State detection of SiO^+ was performed destructively using single-photon resonance-enhanced photodissociation spectroscopy via the predissociative $C^2\Pi$ state, which our preliminary linewidth measurements indicate has a lifetime of order of several hundred picoseconds for $v=0$ and less for higher v. These lifetimes are sufficiently long to provide rotational resolution and sufficiently short for efficient dissociation. The state was previously reported in theoretical studies as the $2^2\Pi$ state [32–34,44,45]. It had not been observed experimentally prior to this work. A manuscript detailing spectroscopy of the $C^2\Pi$ state is currently in preparation [46].

A pulsed dye laser with frequency-doubled output near 226 nm was used for dissociation. Predissociation of SiO^+ via the $C^2\Pi$ state leads to $Si^+ + O$ products, and we monitored the LCFMS SiO^+ signal to measure the dissociated fraction. We performed two types of measurements to characterize state control.

The first method uses slow steady-state depletion, where the rate constant yields relative populations. The LCFMS signal was monitored while optical pumping and concurrently firing the 10 Hz dissociation laser tuned to frequency f for 30 s. If dissociation is slow enough, steady-state population is maintained, and the number of SiO^+ molecules as a function of pulse number m is given by $N_{SiO^+}=N_0e^{-\Gamma(f)m}$. Each pulse dissociates a fraction of remaining molecules given by

$$d(f)=p_N(f)n_N\approx-\frac{dN_{SiO^+}}{dm}\frac{1}{N_{SiO^+}}=\Gamma(f), \qquad (1)$$

where $p_N(f)$ is the probability per pulse of dissociating a molecule which is in the probed state N, and n_N is the fraction of remaining molecules in that state. To ensure that Eq. (1) is valid, we require $p_N(f)\ll 1$ and $\Gamma\ll\Gamma_{eq}$, where Γ_{eq} is the equilibration rate of the probed state. Experimentally, we reduce the dissociation laser fluence until these conditions are met. A fit to the LCFMS decay at each f yields the dissociation spectrum $d(f)$, in which the peak heights depend both on line strength and population. Although these spectra show only relative populations, this first method provides a good signal-to-noise ratio (SNR), since the entire sample contributes toward statistics even for probed states with low population. Also, spectra can be taken with constant SNR over a dynamic range of more than two orders of magnitude.

The second method is a single-shot depletion technique [20,21,41], which yields absolute populations. We recorded the LCFMS signal before and after a single intense pulse tuned to dissociate from state N, where $p_N(f)\sim 1$. Because the predissociation lifetime of the upper state is much shorter than the 10 ns pulse duration, 100% dissociation probability is achievable. The fractional population in N is given by $F_N=(D_i-D_f)/D_i$, where D_i and D_f are the (positive-valued) LCFMS fractional fluorescence dips before and after the dissociation pulse.

Relative cooling efficiency.—Figure 1(c) shows the dipole-allowed $|X^2\Sigma^+, v=0\rangle \rightarrow |C^2\Pi_{3/2}, v=1\rangle$ dissociative readout transitions. This vibronic transition was chosen because it exhibits good separation between lines originating from $N=0$ and $N=1$ as well as from other isotopologues. Each originating N has up to four resolvable lines labeled as $x(N)$. The branch type x is characterized by $\Delta N=(J'+1/2)-N$, where J' is the upper rotational quantum number; e.g., ${}^sR_{21}(0.5)$ is denoted $s(0)$.

Figure 3 shows the spectrum after the population has been pumped toward $N=0$. We simulated the spectrum using PGOPHER [47] and fit the spectral envelope to obtain a ratio of population in $N=1$ to $N=0$ of 0.075(3). We also demonstrate cooling into an excited rotational state by applying the spectral mask for $N=10$ (Fig. 2). Both the $N=0$ and $N=10$ spectra are in sharp contrast with a thermal distribution at 300 K.

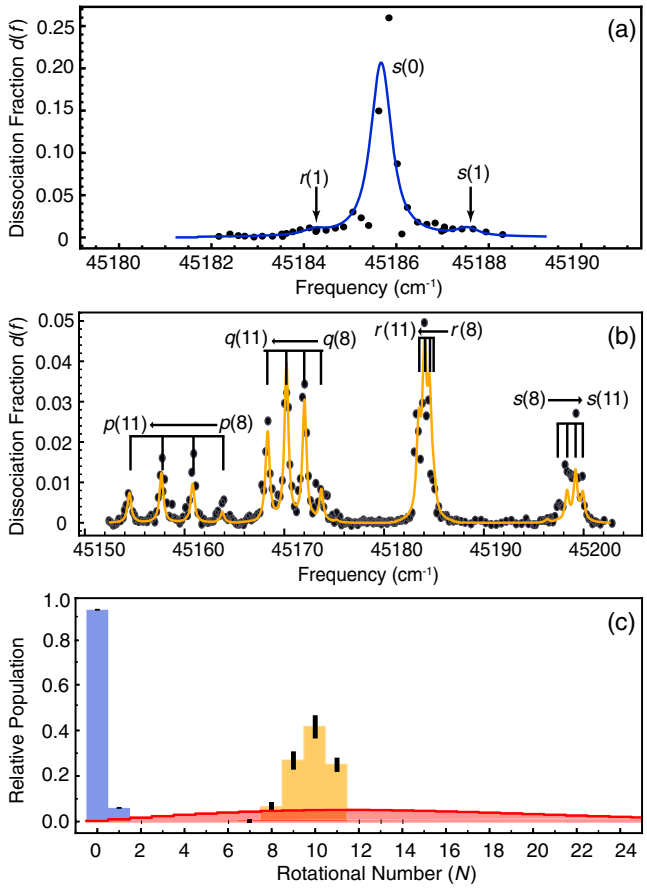

FIG. 3. Dissociation spectra of SiO^+ optically pumped (a) towards $N = 0$ and (b) $N = 10$. (c) Relative rotational state populations inferred from the spectra and their $\pm 1\sigma$ uncertainties, along with a 300 K thermal distribution (red).

Although the steady-state analysis technique does not directly yield absolute populations, some qualitative conclusions can be drawn about populations in other states. Scans searching for transitions originating from $N \geq 2$ of $v = 0$ and for any N of $v = 1$ did not show any discernable peaks. The states in the $A^2\Pi$ manifold are too short lived for significant population accumulation. A quantitative measurement setting bounds on these and other populations is discussed in the section below.

Absolute cooling efficiency and timescale.—Figure 4 shows the measured population accumulation in $N = 0$ when pumping toward that state, analyzed using the single-shot method. Here, we used the $|X^2\Sigma^+, v = 0, N = 0\rangle \rightarrow |C^2\Pi_{1/2}, v = 0, J = 0.5\rangle$ transition at 44 044.5 cm^{-1}. Technical noise, which dominates over SiO^+ counting noise, is primarily due to laser fluctuations affecting Ba^+ cooling efficiency and fluorescence. The anomalous point at very short times is understood to be a spurious signal from population in $N = 11$, which has an overlapping line.

Two timescales are present. The faster timescale is for cooling of the separate parity populations independently. Photon absorption and then spontaneous emission on the diagonal B-X transitions is a parity-preserving process, so approximately half of the population is unable to be directly pumped into the even-parity ground rotational state. The slower timescale is determined by the rate of parity flips. The details of this process have not been determined, but one possible pathway for obtaining the requisite odd number of electric dipole transitions is shown in Fig. 1(a) (also see the Supplemental Material [48]).

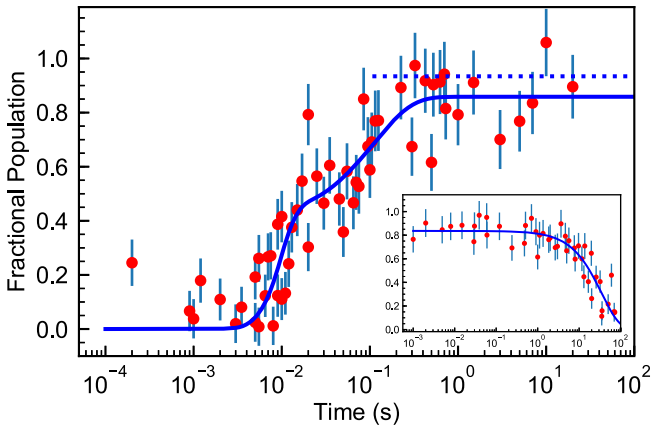

FIG. 4. Single-shot analysis of $N = 0$ population versus optical pumping time. Error bars account for technical noise and SiO^+ counting statistics. Since LCFMS involves difference measurements, points and error bars outside of the range of 0 to 1 are expected. The solid line is a fit to the model, and the horizontal line indicates the corrected asymptote accounting for systematic shifts. Inset: measured longevity of molecules prepared in $N = 0$, after the pumping laser is turned off.

An analytic model (see the Supplemental Material [48]) is used to fit the data. To assess absolute cooling efficiency, an offset must be applied to correct systematic shifts from reaction with the background hydrogen [51], isotopic impurities, and partial overlap of the laser linewidth with other dissociating transitions. We conclude that the steady-state $N = 0$ absolute population fraction of $^{28}Si^{16}O^+$ is 0.94 (3), which corresponds to a temperature of 0.53(6) K. This result is in good agreement with the relative population analysis.

Thermalization of SiO^+ out of $N = 0$, after the cessation of optical pumping, is shown in the inset of Fig. 4. The population loss is well fit by an exponential decay with a time constant of 35(4) s. This timescale is much faster than blackbody-induced pure rotational (400 s) or vibrational excitations (380 s), and also faster than the observed reaction rate with H_2 (~600 s). However, it could be consistent with inelastic collisions with H_2 [51], which have a Langevin collision time of 40(20) s, with uncertainty coming from the H_2 pressure. Blackbody redistribution via the A state is also a possible mechanism, expected to occur on a time scale of 70–130 s given the predicted A state lifetimes [34,37].

Conclusions.—This work demonstrates the extension of a broadband rotational cooling technique from a trapped

diatomic hydride to an oxide. Furthermore, we show that the class of diagonal molecules amenable to rotational cooling can be extended to include those with an intermediate electronic state not involved in the dominant optical pumping cycle.

Higher resolution spectral filtering is possible, for example by using a virtual imaged phased array (VIPA) where sub-GHz resolution has been achieved [48,52]. VIPA could significantly enhance the preparation fidelity of the $N = 0$ and $N = 10$ states shown here. Consequently, it might be advantageous to use $N > 0$ states for quantum information processing, since dominant decoherence mechanisms are reduced for higher rotational states [12]. Optical pumping to $N \gg 0$, not explored in this work, can also be useful for spectroscopic studies and can provide insights into the molecular Hamiltonian at high energies [46].

The limiting timescale is currently the parity cooling step. Electronic decay from A to X is predicted to be of order 5 ms [34], thus we expect that the cooling rate could be increased by more than an order of magnitude with increased spectral fluence of the pump laser. An alternative would be to use microwaves to drive parity flips, for instance at 86 GHz connecting $N = 1$ with $N = 2$ [53,54] for cooling to $N = 0$. Use of a microwave drive could equalize the timescales for cooling the two parities, and with a more intense cooling laser $^{28}Si^{16}O^+$ population could be cooled to a pure internal quantum state in $< 10\ \mu s$, limited by the spontaneous emission rate of B. Further refinements may enable fluorescence imaging or direct Doppler cooling of SiO^+ [34,37] and could help realize multi-ion molecular clocks with canceling Stark and second order Doppler shifts [55].

We have demonstrated straightforward pumping of $^{28}Si^{16}O^+$ to a state of well-defined angular momentum. Since $^{28}Si^{16}O^+$ also has microwave-accessible rotational transitions for quantum manipulation, this species could play a similar role in a wide range of applications, as do only a relatively small handful of popular atomic species.

We gratefully acknowledge Jason Nguyen for proposing rotational cooling of SiO^+, along with his and David Tabor's early work on SiO^+ in the lab. Development of dissociative analysis techniques were funded by NSF Grant No. PHY-1806861, LCFMS techniques were funded by ARO Grant No. W911NF-14-0378, and optical state control techniques were funded by AFOSR Grant No. FA9550-17-1-0352.

*These authors contributed equally to this work.
†b-odom@northwestern.edu

[1] M. T. Bell, A. D. Gingell, J. M. Oldham, T. P. Softley, and S. Willitsch, Faraday Discuss. **142**, 73 (2009).
[2] A. D. Dörfler, P. Eberle, D. Koner, M. Tomza, M. Meuwly, and S. Willitsch, Nat. Commun. **10**, 5429 (2019).
[3] M. T. Bell and T. P. Softley, Mol. Phys. **107**, 99 (2009).
[4] J. M. Hutson, Science **327**, 788 (2010).
[5] N. Balakrishnan, J. Chem. Phys. **145**, 150901 (2016).
[6] W. S. Ian, *Low Temperatures and Cold Molecules* (World Scientific, Singapore, 2008).
[7] B. Yan, S. A. Moses, B. Gadway, J. P. Covey, K. R. A. Hazzard, A. M. Rey, D. S. Jin, and J. Ye, Nature (London) **501**, 521 (2013).
[8] K. R. A. Hazzard, B. Gadway, M. Foss-Feig, B. Yan, S. A. Moses, J. P. Covey, N. Y. Yao, M. D. Lukin, J. Ye, D. S. Jin *et al.*, Phys. Rev. Lett. **113**, 195302 (2014).
[9] R. Schmidt and M. Lemeshko, Phys. Rev. Lett. **114**, 203001 (2015).
[10] R. Schmidt and M. Lemeshko, Phys. Rev. X **6**, 011012 (2016).
[11] K.-K. Ni, T. Rosenband, and D. D. Grimes, Chem. Sci. **9**, 6830 (2018).
[12] E. R. Hudson and W. C. Campbell, Phys. Rev. A **98**, 040302 (R) (2018).
[13] W. C. Campbell and E. R. Hudson, arXiv:1909.02668 [Phys. Rev. Lett. (to be published)].
[14] M. S. Safronova, D. Budker, D. DeMille, D. F. J. Kimball, A. Derevianko, and C. W. Clark, Rev. Mod. Phys. **90**, 025008 (2018).
[15] W. B. Cairncross, D. N. Gresh, M. Grau, K. C. Cossel, T. S. Roussy, Y. Ni, Y. Zhou, J. Ye, and E. A. Cornell, Phys. Rev. Lett. **119**, 153001 (2017).
[16] V. Andreev, D. G. Ang, D. DeMille, J. M. Doyle, G. Gabrielse, J. Haefner, N. R. Hutzler, Z. Lasner, C. Meisenhelder, B. R. OLeary *et al.*, Nature (London) **562**, 355 (2018).
[17] S. Alighanbari, G. S. Giri, F. L. Constantin, V. I. Korobov, and S. Schiller, Nature (London) **581**, 152 (2020).
[18] C. W. Chou, A. L. Collopy, C. Kurz, Y. Lin, M. E. Harding, P. N. Plessow, T. Fortier, S. Diddams, D. Leibfried, and D. R. Leibrandt, Science **367**, 1458 (2020).
[19] M. Viteau, A. Chotia, M. Allegrini, N. Bouloufa, O. Dulieu, D. Comparat, and P. Pillet, Science **321**, 232 (2008).
[20] P. F. Staanum, K. Højbjerre, P. S. Skyt, A. K. Hansen, and M. Drewsen, Nat. Phys. **6**, 271 (2010).
[21] T. Schneider, B. Roth, H. Duncker, I. Ernsting, and S. Schiller, Nat. Phys. **6**, 275 (2010).
[22] A. Cournol, P. Pillet, H. Lignier, and D. Comparat, Phys. Rev. A **97**, 031401(R) (2018).
[23] C.-Y. Lien, C. M. Seck, Y.-W. Lin, J. H. Nguyen, D. A. Tabor, and B. C. Odom, Nat. Commun. **5**, 4783 (2014).
[24] W. G. Rellergert, S. T. Sullivan, S. J. Schowalter, S. Kotochigova, K. Chen, and E. R. Hudson, Nature (London) **495**, 490 (2013).
[25] A. K. Hansen, O. Versolato, S. B. Kristensen, A. Gingell, M. Schwarz, A. Windberger, J. Ullrich, J. C. López-Urrutia, M. Drewsen *et al.*, Nature (London) **508**, 76 (2014).
[26] X. Tong, A. H. Winney, and S. Willitsch, Phys. Rev. Lett. **105**, 143001 (2010).
[27] C.-w. Chou, C. Kurz, D. B. Hume, P. N. Plessow, D. R. Leibrandt, and D. Leibfried, Nature (London) **545**, 203 (2017).
[28] Y. Shagam and E. Narevicius, J. Phys. Chem. C **117**, 22454 (2013).
[29] K.-K. Ni, S. Ospelkaus, M. De Miranda, A. Pe'Er, B. Neyenhuis, J. Zirbel, S. Kotochigova, P. Julienne, D. Jin, and J. Ye, Science **322**, 231 (2008).

[30] U. Bressel, A. Borodin, J. Shen, M. Hansen, I. Ernsting, and S. Schiller, Phys. Rev. Lett. **108**, 183003 (2012).
[31] H.-J. Werner, P. Rosmus, and M. Grimm, Chem. Phys. **73**, 169 (1982).
[32] Z.-L. Cai and J.-P. François, J. Mol. Spectrosc. **197**, 12 (1999).
[33] S. Chattopadhyaya, A. Chattopadhyay, and K. K. Das, J. Mol. Struct. THEOCHEM **639**, 177 (2003).
[34] R. Li, X. Yuan, G. Liang, Y. Wu, J. Wang, and B. Yan, Chem. Phys. **525**, 110412 (2019).
[35] M. D. Di Rosa, Eur. Phys. J. D **31**, 395 (2004).
[36] D. Sofikitis, S. Weber, A. Fioretti, R. Horchani, M. Allegrini, B. Chatel, D. Comparat, and P. Pillet, New J. Phys. **11**, 055037 (2009).
[37] J. H. V. Nguyen and B. Odom, Phys. Rev. A **83**, 053404 (2011).
[38] J. H. V. Nguyen, C. R. Viteri, E. G. Hohenstein, C. D. Sherrill, K. R. Brown, and B. Odom, New J. Phys. **13**, 063023 (2011).
[39] P. R. Stollenwerk, B. C. Odom, D. L. Kokkin, and T. Steimle, J. Mol. Spectrosc. **332**, 26 (2017).
[40] Y.-W. Lin and B. C. Odom, arXiv:1610.04324.
[41] C.-Y. Lien, S. R. Williams, and B. Odom, Phys. Chem. Chem. Phys. **13**, 18825 (2011).
[42] P. R. Stollenwerk, I. O. Antonov, and B. C. Odom, J. Mol. Spectrosc. **355**, 40 (2019).
[43] T. Baba and I. Waki, J. Appl. Phys. **89**, 4592 (2001).
[44] N. Honjou, Mol. Phys. **101**, 3063 (2003).
[45] D. Shi, W. Li, W. Xing, J. Sun, Z. Zhu, and Y. Liu, Comput. Theor. Chem. **980**, 73 (2012).
[46] I. O. Antonov, P. R. Stollenwerk, S. Venkataramanababu, A. P. de Lima Batista, A. G. S. de Oliveira Filho, and B. C. Odom, arXiv:2008.01904.
[47] C. M. Western and B. E. Billinghurst, Phys. Chem. Chem. Phys. **21**, 13986 (2019).
[48] See the Supplemental Material at http://link.aps.org/supplemental/10.1103/PhysRevLett.125.113201 for further discussion of possibilities for tailored spectra, which includes Refs. [49,50].
[49] R. Horchani, Opt. Quantum Electron. **47**, 3023 (2015).
[50] P. R. Stollenwerk, Ph.D. thesis, Department of Physics Northwestern University, 2020.
[51] D. Fahey, F. Fehsenfeld, E. Ferguson, and L. Viehland, J. Chem. Phys. **75**, 669 (1981).
[52] J. T. Willits, A. M. Weiner, and S. T. Cundiff, Opt. Express **20**, 3110 (2012).
[53] S. D. Rosner, R. Cameron, T. J. Scholl, and R. A. Holt, J. Mol. Spectrosc. **189**, 83 (1998).
[54] T. J. Scholl, R. Cameron, S. D. Rosner, and R. A. Holt, Can. J. Phys. **73**, 101 (1995).
[55] P. R. Stollenwerk, M. G. Kokish, A. G. S. de Oliveira-Filho, F. R. Ornellas, and B. C. Odom, Atoms **6**, 53 (2018).